Received: 27 October 2020 | Accepted: 29 October 2020

DOI: 10.1002/pls2.10021

RESEARCH ARTICLE

SPE POLYMERS WILEY

Development, characterization and modeling of mosquito repellent release from microporous devices

Alcides Sitoe[1,2,3] | **António B. Mapossa**[1,2] | **Walter W. Focke**[1,2] | **Herminio Muiambo**[3] | **René Androsch**[4] | **James Wesley-Smith**[5]

[1]Institute of Applied Materials, Department of Chemical Engineering, University of Pretoria, Pretoria, South Africa

[2]UP Institute for Sustainable Malaria Control & MRC Collaborating Centre for Malaria Research, University of Pretoria, Pretoria, South Africa

[3]Department of Chemistry, Eduardo Mondlane University, Maputo, Mozambique

[4]Interdisciplinary Center for Transfer-oriented Research in Natural Sciences, Martin Luther University Halle-Wittenberg, Halle/Saale, Germany

[5]Electron Microscope Unit, Sefako Makgatho Health Sciences University, Ga-Rankuwa, South Africa

Correspondence
Alcides Sitoe, Institute of Applied Materials, Department of Chemical Engineering, University of Pretoria, Lynnwood Road, Pretoria, South Africa.
Email: alcides.sitoe@gmail.com

Funding information
Deutsche Forschungsgemeinschaft, Grant/Award Number: Grant AN 212/22-1

Abstract

Nanocomposite strands with mosquito repellent DEET or Icaridin incorporated in a poly(ethylene-co-vinyl acetate) (EVA) matrix, with either pyrogenic silica or an organoclay as a nanofiller, were prepared by a twin-screw extrusion compounding technique. The nature and levels of the repellent and nanofiller that was used affected the material phase morphology. The repellent release was followed as a function of aging time in convection ovens set at 30 and 50°C. The experimental release data of the mosquito repellent from the microporous polymer swellable matrix strands was mathematically modeled and fitted using a range of semi-empirical models. In the majority of case, the Korsmeyer-Peppas power law model provided the best data fit. As expected, the wide range of internal morphologies also resulted in quite different release profiles. These models were found to be valuable as they provided insights into the mechanism of repellent release from EVA swellable matrices. It was possible to differentiate between diffusion and relaxation mechanisms. Surprisingly, strands containing nominally more than 30 wt% Icaridin showed accelerating mass loss during the initial phase, consistent with Super Case II transport. Diffusional exponents as high as 1.81 were found. Furthermore, the internal microporous region of the extruded EVA strands was covered by a surface membrane that acted a diffusion barrier that, in effect, controlled the release rate of the mosquito repellents. Some of the investigated samples exhibited release profiles that suggest that longer lasting effective release of repellents is possible than currently achieved by available commercially products.

KEYWORDS

controlled release, microporous system, modeling, repellent

1 | INTRODUCTION

Collectively, the mosquito-borne diseases of malaria, Dengue, Yellow fever, O'nyong-nyong fever, Zika and lymphatic filariasis (elephantiasis) are the single biggest cause of morbidity and mortality in humans. These mosquito-transmitted infections occur at the global scale and involve a wide range of viral and other pathogenic

agents. Female mosquitoes require a blood meal for optimal egg-maturation. The pathogens are taken up when a female mosquito feeds on a human host and she transmits them to another human during a subsequent feed.[1–3] The World Health Organization (WHO) recommended vector control interventions include indoor residual spray (IRS) and long-life insecticidal bed nets (LLINs). However, LLINs and IRS protect only against indoor biting and resting mosquitoes. It is still possible for people to be infected whilst outdoors.

Many mosquito species, for example, *An. arabiensis*, *An. gambiae s.s.* and *An. funestus*, are strongly attracted by human foot odor. They tend to bite victims in the ankle area especially when outdoors.[4,5] This is strikingly illustrated in Figure 1. Wearing mosquito-repellent polymer-foot bracelets might reduce infective lower limb bites and thereby help to reduce the overall disease transmission rates. The affordability of such personal protection devices is an important consideration in Third World countries. Fortunately, it appears possible to increase the duration of repellence activity by incorporating repellents into inexpensive thermoplastic polymers, for example, linear low-density polyethylene (LLDPE) or poly(ethylene-co-vinyl acetate) (EVA).[6] The EVA holds an advantage over the LLDPE as it yields softer strands that promise a more comfortable wearing experience. Laboratory testing confirmed that EVA strands that contain 20 or 30 wt% of either DEET or Icaridin can provide effective protection against mosquito bites even after 12 weeks of aging at 50°C.[6]

Repellents need to be released into the surrounding air to be effective, that is, they are continuously lost to the atmosphere. This means that long-life bracelets should also need to act as reservoirs for relatively large quantities of the active compound. It proved possible to trap repellent amounts in polymer matrices that significantly exceed the solubility limit at ambient temperatures.[6] One way is to force phase separation by spinodal decomposition to induce a co-continuous phase structure with the liquid repellent trapped inside the pores defined by the polymer scaffold.[7] Such open-cell foam phase structures are relatively easy to obtain by extruding hot homogeneous polymer-repellent melts into an ice-cold water bath. In the case of LLDPE as scaffold, the solubility of the polar repellent in the nonpolar semi-crystalline polymer is very low. This facilitated the formation of an open-cell morphology for the polymer scaffold. Another feature observed with polyethylene as matrix polymer, is the formation of a thin integral skin layer on the outside of the extruded strands. It turns out that the release of repellent from such polyethylene strands is well-described by a mechanistic model that incorporates this outer membrane as the dominant diffusional mass transfer barrier.[6]

The ultimate goal is the design and development of commercially viable personal protection devices. The temporal release profile of the volatile repellents is an important factor as it affects the length of the effective protection. EVA is more polar than LLDPE and therefore more compatible with the typically polar repellents. Consequently, the phase separation may instead yield liquid repellent-rich phase domains trapped inside a solid polymer-rich matrix phase. Strands made from EVA as polymer matrix showed repellent release behavior that did not conform to the model developed for polyethylene. It was therefore important to gain a better understanding of repellent release profiles from EVA matrices. This is the primary objective of the present communication. It reports on the structure and active release performance of mosquito repellent-containing EVA strands prepared by twin-screw extrusion compounding. The strands contained up to 30 wt% of either DEET or Icaridin.

FIGURE 1 Many mosquitoes show a tendency to bite human hosts in the ankle area. Photo courtesy of mark Lantham

2 | MATERIALS AND METHODS

2.1 | Materials

The mosquito repellent *N*,*N*-diethyl-3-methylbenzamide (DEET) [CAS No. 134–62-3] was obtained from Sigma-Aldrich. It had a purity of ≥97% and a density of 0.998 g cm^{-3} at 20°C. 1-(1-methylpropoxycarbonyl)-2-(2-hydroxyethyl)piperidine (Icaridin) [CAS No. 119515–38-7] was supplied by Saltigo. According to the supplier, the purity exceeded 97%, the boiling point was 272°C and the density is 1.0362 g cm^{-3} at 20°C. Dichloromethane [CAS No. 75–09-2] of purity is 99.9% was obtained from Merck.

Poly(ethylene-co-vinyl acetate) (EVA) (grade Elvax 760A ex DuPont) pellets were pulverized by Dreamweaver. The VA content was 9%, the density 0.930 g cm^{-1} and the melt flow index (MFI) was 2.0 g/10 min (190°C/2.16 kg).

Pyrogenic nanosilica powder HDK N20 was obtained from Wacker Chemie. According to the manufacturer, the silica was amorphous and had a surface area of about 200 m^2 g^{-1}. Laviosa Chimica Mineraria S.p.A. supplied Dellite 43B clay with approximate medium particle size of 8 μm. This clay was organo-modified by intercalation with dimethyl benzyl hydrogenated tallow ammonium. The nanosilica and the clay facilitated the feeding, via the hopper of the extruder, and contributed to rapid mixing and dissolution of the repellents in the polymer melt. Also, the addition of nanofiller can adjust or help to control the repellent-release rate to low values that can provide long-term repellence efficacy.

2.2 | Methods

2.2.1 | Extrusion compounding

A total of 5 wt% organoclay or silica was included in the majority of the formulations to thicken the liquid repellent, even partially solidifying it, in order to assist feeding of the mixture via the hopper into the compounding extruder. The extrusion compounding was performed on a TX28P 28 mm (manufactured by CFAM Technologies [Pty] Ltd, Potchefstroom, South Africa) co-rotating twin-screw laboratory extruder with a screw diameter of 28 mm and an L/D ratio of 18. The screw design of this machine comprised intermeshing kneader blocks that also impart a forward transport action.

The polymer and clay powders were mixed together the repellent in a plastic container to obtain a semi-dry consistency that could be fed into the compounding extruder. Table S1 provides a full list of the formulations prepared. The temperature profiles, from hopper to die, were set at 140/160/160/160°C. The screw speed was varied from 105 to 150 rpm. The exiting polymer strands were quench-cooled in an ice-water bath. The strands diameters produced for the different formulations ranged from 3.2 to 6.4 mm. The diameters of polymers strands were measured with a Mitutoyo Digital Caliper. The reported strand diameters represent averages of five separate measurements.

2.2.2 | Absorption of repellent by the polymers

Approximately 4 g of neat EVA pellets were weighed and placed in Polytop glass vials containing approximately 16 ml DEET or Icaridin. The vials were placed in a forced convection oven set at a temperature of 30 or 50°C. After 3 days, the pellets were removed, and the excess repellent was removed using a quick rinse with dichloromethane. The repellent absorption was estimated from the recorded mass gain of the pellets.

2.2.3 | Repellent content

Polymer strands containing repellents were cut into approximately 70 mm lengths, weighed and placed in tall Polytop glass vials. Approximately 40 ml dichloromethane was added, and the vials were stoppered. The extraction solvent was replaced daily. After the fifth extraction, the strands were removed and allowed to dry in a fume hood at ambient temperature. The repellent content was estimated from the recorded mass loss of the strands in the fully dry form. Reported values are the results obtained from triplicate mass loss determinations.

The repellent content of the polymer strands was also estimated from mass loss recorded in thermogravimetric analysis (TGA). TGA runs were performed on a TA Instruments SDT-Q600 Simultaneous TGA/DSC. Samples, weighing approximately 16 mg, were heated from ambient temperature to 600°C at a rate of 10 K min^{-1}. The purge gas was nitrogen flowing at 50 ml min^{-1}. The first TGA mass-loss step was associated with the evaporative loss of the repellent.

2.2.4 | Scanning electron microscopy (SEM)

Repellent-free polymer strands were immersed in liquid nitrogen for approximately 1 h before fracturing. The fracture surface was rendered conductive by coating with carbon using an Emitech K950X coater prior to analysis. The samples were viewed using a Zeiss Ultra 55 Field Emission Scanning Electron Microscope at acceleration voltages of 1 and 5 kV. In an alternative approach, the strands were cooled to −120°C, trimmed and cryo-planed to a median, smooth block-face using a Leica FC7 ultramicrotome. After warming to room temperature, samples were subsequently mounted on aluminium stubs, rendered conductive by coating and the smooth block faces examined using a Zeiss Supra 55 Field Emission SEM at 2 kV.

2.2.5 | Repellent release

Repellent release was studied by aging at 30 and 50°C in an EcoTherm-Labcon forced convection oven. Samples

strands were cut into 3.0 m lengths and suspended from the inside roof of the ovens in the form of loose coils. The strands were weighed twice a week. The oven aging was continued for up to 12 weeks.

3 | MODELING REPELLENT RELEASE

Increasing attention is being devoted to the way the drugs are delivered. According to Langer and Peppas,[8] ethylene-vinyl acetate copolymer and various hydrogels were most successful in this regard. Schneider, Langer, Loveday and Hair[9] state that ethylene-vinyl acetate copolymers gained prominence due to their broad applicability, long sustained release time scales and highly favorably inflammatory characteristics. Ethylene-vinyl acetate copolymer as polymeric carrier proved to be suitable material for drug release for different purposes.[9–14]

In an amorphous polymer, dynamic swelling controls the solute diffusion in most cases. The mechanism involves diffusional release from the continuously swelling or shrinking system.[15–18]

In swelling controlled-release systems, the release of a solute is controlled by one or more of the following processes: namely, the transport of the solvent into the polymer matrix, swelling of the associated polymer, diffusion of the solute through the swollen polymer, erosion of the swollen polymer and so forth. Controlled release from swellable polymeric systems has been studied extensively and numerous models were proposed. These have been reviewed from time to time by several researchers.[19–32] However, there is no single model that successfully predicts all possible experimental conditions. Nevertheless, collectively they can contribute towards the elucidation of the mechanism involved.

Figure 2 shows schematically, in cross-section, two possible phase morphologies of repellent-filled polymer strands. Figure 2(A) corresponds to the situation where a dense outer skin covering controls the release of repellent from an open-cell inner structure, partially filled with liquid repellent. The strands obtained from LLDPE approximated to this situation. The time dependent release from such strands followed the predictions of a simple implicit mechanistic model[6]:

$$t/\tau = \beta X + (1-X)\ln(1-X) \quad (1)$$

where $X = m(t)/m(t \to \infty)$ is the fraction of repellent mass (m) released after elapsed time (t) normalized with respect to the maximum that can be released; the characteristic time τ and the shape parameter β both depend on geometric factors and the physical properties of the

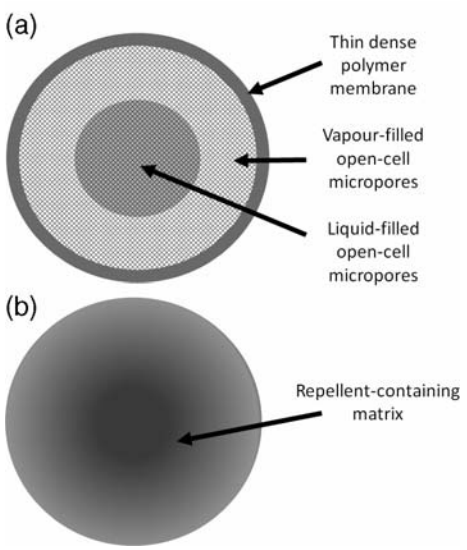

FIGURE 2 Cross-section of repellent-containing strands. (A) Open-cell microporous matrix with integral skin controlling the release. (B) Liquid-swollen polymer matrix with a radial repellent concentration gradient

repellent and the polymer matrix. The model defined by Equation (1) assumes quasi-steady state diffusion and a dimensionally stable and inert solid scaffold. This means that it will break down if the polymer absorbs and swells in the presence of the repellent. This is expected to be the case for EVA as this polymer is more polar than polyethylene. Indeed, it was observed that in some cases the repellent release profiles from EVA matrices were such that they could not be modeled with Equation (1).

The release of mobile actives from swelling polymeric systems belongs to the category of diffusion problems known as moving-boundary or Stefan-Neumann problems.[33] Closed-form solutions are not generally available, and it has become common practice to employ semi-empirical models to fit experimental data. The most widely applied models are due to Peppas and coworkers.[33–36] They realized that the behavior of such systems is determined by two competing release mechanisms, that is, Fickian diffusion and a Case II relaxation process. On this basis they developed two important semi-empirical release models on heuristic grounds.[34] They observed that, regardless of the geometric shape of the release device, the first 60% of a release curve is adequately described by the so-called Korsmeyer-Peppas power law model[36]:

$$X(t) = (t/\tau)^n \quad (2)$$

where again τ is a characteristic time constant, t is the release time and n is the diffusional exponent for active release. Typical values of the latter, are shown in Table 1.

Peppas and Sahlin[35] proposed an additive model to describe combined Fickian and Case II diffusion. They simply summed the two limiting exponential expressions of solute release from polymeric devices, that is, the release mechanism's diffusion and relaxation contributions. For example, the Peppas-Sahlin model for release from infinite cylinders is given by

$$X(t) = (t/\tau_1)^{0.45} + (t/\tau_2)^{0.89} \quad (3)$$

The disadvantage of the Korsmeyer-Peppas and Peppas-Sahlin models is that they only describe the initial portion of the release profile. The log-logistic model provides a recognizable generalization to the Korsmeyer-Peppas model valid over the full release range:

$$X(t) = (t/\tau)^n/[1 + (t/\tau)^n] \quad (4)$$

This model represents the solution to a rate expression in which the exponent n affords a parametric interpolation between the predictions of the logistic equation ($n \to 0$) and second order kinetics ($n = 1$).[38]

The Weibull's model provides another globally valid expression for modeling release rates:

$$X(t) = 1 - \exp[-(t/\tau)^n] \quad (5)$$

This expression is highly flexible and capable of correlating the behavior of complex diffusion systems[18] including diffusion in fractal and disordered substrates.[39] The dimensionless exponent n is a shape parameter that determines the nature of the release curve. Interestingly the Weibull's model also constitutes an extension of the Korsmeyer-Peppas model. This is because the exponent n is linearly related to the exponent n of the power law derived from the analysis of the first 60% of a release curve.[39] Furthermore, the value that the exponent n serves as an indicator of the mechanism of transport of the active through the polymer matrix.[39] Values of $n \leq 0.75$ indicate Fickian diffusion in either fractal or Euclidian spaces.[39] Values in the range $0.75 < n < 1$ are associated with a combined mechanism (Fickian diffusion and Case II transport). If $n = 1$, the Weibull's model reduces to classical first-order kinetics.[16] Complex release mechanisms are indicated when the n value exceeds unity.[40,41]

Ideally, the repellent release rate should be constant and just above the effective level. This will guarantee the longest effective application time. This implies zero order release kinetics corresponding to a linear release profile, that is, $n = 1$ for the diffusional exponent of the Korsmeyer-Peppas expression. It turns out that it is in principle possible for this ideal to be approached regardless of the device geometry.[34,42]

The exponential dependence of the amount of drug released on time, as described by Korsmeyer-Peppas power law model, can still be used for the analysis of swelling-controlled release systems as long as these systems swell only moderately in the solute. The first estimate of applicability of this equation in swellable systems is that the system does not swell more than 25% of its original volume.[33]

4 | RESULTS AND DISCUSSION

4.1 | Absorption of repellent by the polymers

The ultimate target is to produce long-life repellent bangles or anklets. It was important to estimate the degree of shrinkage of the polymer matrix strands containing repellents. According to Akhtar and Focke,[7] this dimensional instability is undesirable in products, such as insect repellent wearable devices. Swelling of the polymer strands implies the possibility of shrinkage when the repellent is released. Excessive shrinkage could lead to discomfort and even constriction of the limbs. Table 2 lists the relative quantities of repellent that were absorbed by EVA polymer at 30 and 50°C. At both temperatures, less Icaridin was absorbed than DEET. Fortunately, the swelling was not excessive which means that shrinkage of anklets based on these formulations is unlikely to be problematic.

The results are in agreement with those observed by Charara, Williams, Schmidt, and Marshall[43] studying the absorption of EOs in various polymeric packaging

TABLE 1 The values of the diffusional exponent applicable to different geometries and different limiting transport mechanisms[35,37]

Infinite thin sheet	Infinite cylinder	Sphere	Mechanism
0.5	0.45	0.43	Case I: Fickian diffusion
$0.5 < n < 1$	$0.45 < n < 0.89$	$0.43 < n < 0.85$	Anomalous transport
1	0.89	0.85	Case II: Non-Fickian diffusion
>1	>0.89	>0.85	Super Case II

materials. They reported that the highest absorption was found in materials with low crystallinity. The semi-crystalline and nonpolar LLDPE reported by Mapossa, Sibanda, Sitoe, Focke, Braack, Ndonyane, Mouatcho, Smart, Muaimbo and Androsch[6] absorbed less polar repellent compared to the amorphous and polar EVA matrix. The polar repellent interacted very weakly with the nonpolar LLDPE matrix compared to EVA that contained the polar group (containing 9% VA). The results show that the solubility of Icaridin was lower compared to DEET, this can suggest that Icaridin was less compatible with the polymer.

4.2 | Repellent content by TGA

Figure 3 shows typical TGA traces obtained for the repellent (Icaridin and DEET), the neat EVA polymer, as well as repellent-filled polymer-clay nanocomposites. The corresponding TGA traces for DEET-filled compositions had a very similar appearance. For the neat Icaridin, mass loss commenced just above 126°C and was complete by 294°C. By contrast, evaporative mass loss of the neat DEET commenced earlier just above 105°C and was complete by 268°C. The first mass loss event for Icaridin is assigned to the volatilization of the repellent component present in the polymer-based strands. The EVA polymer featured the highest thermal stability. Mass loss was a mere 2 wt% when the temperature reached 329°C. Further EVA thermal degradation features two major steps.[44] They are attributed to (i) the loss of vinyl acetate units via a de-acylation process resulting in the formation of double bonds, and (ii) to the degradation of resulting partially unsaturated polyethylene material polymer.[45]

Compared to the neat EVA, the nanocomposites feature an earlier mass loss step. This mass loss event is attributed to the volatilization of the repellent present. Unfortunately, the mass loss curves did not show a clear plateau range that would have made it easy to estimate the repellent content. Instead, the repellent content was evaluated as follows. The difference between the mass loss for the neat EVA and that for the nanocomposite was plotted against temperature as illustrated in Figure 3 (B),(D). Such plots showed a clear maximum, and this

TABLE 2 Effect of repellent nature and temperature on the degree of polymer swelling (%)

Temperature (°C)	DEET	Icaridin
30	1.65 ± 0.14	0.99 ± 0.09
50	5.14 ± 0.10	3.18 ± 0.11

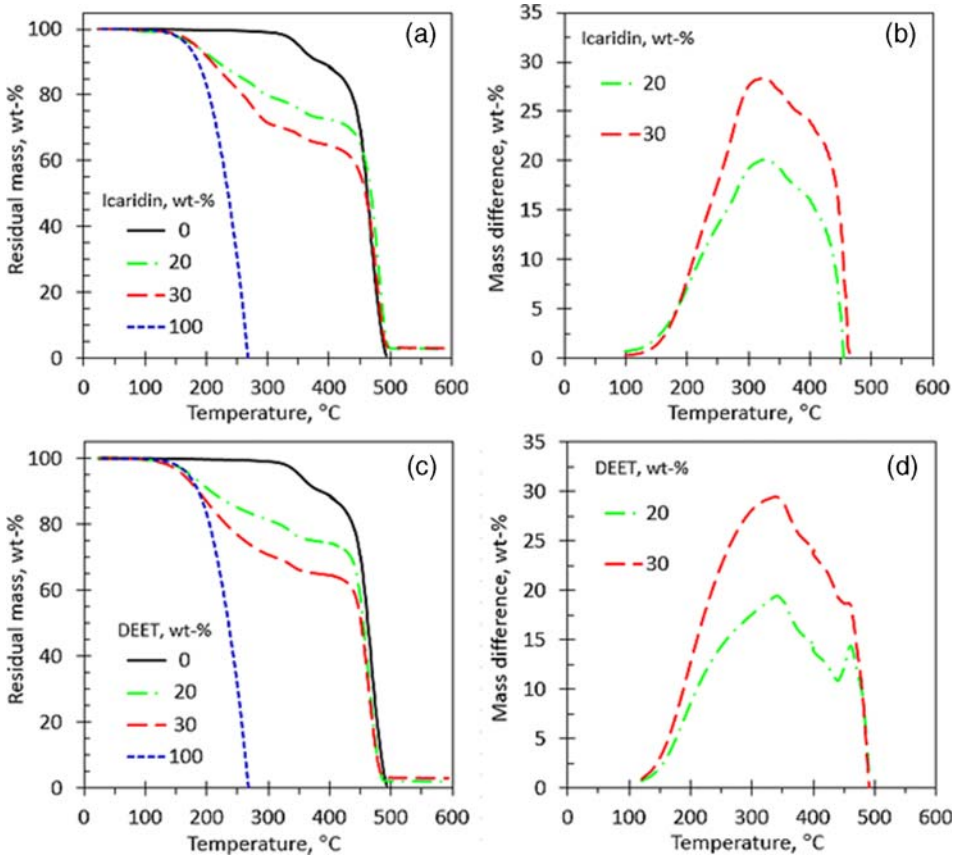

FIGURE 3 (A) TGA mass loss traces for Icaridin, the neat EVA and two Icaridin-filled polymer nanocomposite strands containing 5 wt% Dellite 43B clay obtained in a nitrogen atmosphere. (B) Plot of the difference in mass loss between the EVA and the nanocomposites

was associated with the repellent content of the nanocomposite.

Table 3 compares estimated repellent content values for the nanocomposite as determined by thermogravimetric analysis (TGA) and solvent extraction for a few selected samples. There is good agreement between the values obtained by the two different methods. Additionally, these values are also in reasonable agreement with the nominal repellent contents set during the strand compounding experiments. These results indicate that very little repellent was lost by evaporation during the extrusion-compounding process. More details of the repellent content of all samples studied are presented in the Supporting Information.

4.3 | Morphology by SEM

Figure 4 shows representative SEM micrographs of EVA strands after leaching the repellents with dichloromethane. All samples featured a relatively smooth outer surface as shown in Figure 4(A). However, the internal morphology varied widely depending on the nature and loading level of both the repellent and the nanoparticles that were present. Before leaching, the strands appeared translucent and they assumed an opaque white appearance after leaching. This suggests a porous, foam-like internal structure confirmed by SEM images. However, Icaridin-derived samples appeared dense and pore-free especially when incorporated at low initial loading levels. Figure 4(B) shows such an example in which the dispersed clay platelets are also visible. Figure 4(C) shows the structure obtained with a high DEET loading and with pyrogenic silica as the nanofiller. Silica agglomerates are clearly visible in the opening suggesting that the silica was associated with the repellent rich regions. Figure 4(D) shows a sample that had a lower repellent loading with the organoclay as filler. This sample is consistent with a microporous internal morphology. Additional micrographs are provided in the Supporting Information.

TABLE 3 Nominal repellent content (in wt%) and values estimated using solvent extraction and thermogravimetric analysis (TGA)

Polymer strand	Nominal	TGA	Solvent extraction
EVA-DEET	20	19.5	18.7 ± 0.5
EVA-DEET	30	29.5	29.0 ± 0.2
EVA-Icaridin	20	20.2	19.6 ± 0.2
EVA-Icaridin	30	28.4	30.1 ± 0.5

4.4 | Repellent release profiles

Figures 5–8 show a range of repellent release profiles. Figure 5 shows the effect of nanofiller type and repellent nature on the release of the latter as a function of time. The samples were aged in a convection oven at 30 and 50°C. DEET was released more rapidly than Icaridin irrespective of all other factors. The repellent release was slower from strands containing the organoclay than from strands containing pyrogenic silica. However, strands containing both silica and clay at the 5 wt% level performed similar to the strands containing pyrogenic silica only.

Figure 6 shows the effect of active content on repellent release from EVA strands containing 5 wt% organoclay and aged in a convection oven set at 50°C. As before, DEET was released more rapidly that Icaridin. Surprisingly, the strands containing lower levels of repellent were depleted fastest.

Figure 7 shows the effect of organoclay loading level on repellent release from the EVA strands aged in a convection oven set at 50°C. The strand without clay and the strand made using 1 wt% clay showed similar release profiles. So did the strands containing 2.5 and 5 wt% clay respectively. The repellent release occurred fastest for the former indicating that the presence of clay can reduce the rate of repllent release. Noteworthy is the near constant release rate shown by all these strand containing nominally 20 wt% Icaridin.

Figure 8 shows the effect of strand diameter and oven aging temperature on the release of DEET from EVA strands. As expected, the release is faster from the thinner strands and at the higher aging temperature. The former can be attributed to a larger surface to volume ratio and the latter to the increase in the volatility. The diameter of the thinner strands were about 60% of the thicker ones and this led to an increase in the repellent release by about 40% at comparable aging times. The effect of lowering the temperature from 50 to 30°C had a greater effect. The amount released at the lower temperature was only about 27% of that at the higher temperature at comparable aging times.

4.5 | Modeling repellent release from EVA strands

The release profile data were fitted with different semi-empirical models using a least squares method. Tables S2 and S3 lists the values of the model parameters. The fit quality was superficially assessed based on correlation coefficients. Using this metric, the Korsmeyer-Peppas model gave the best fit more often than the other models.

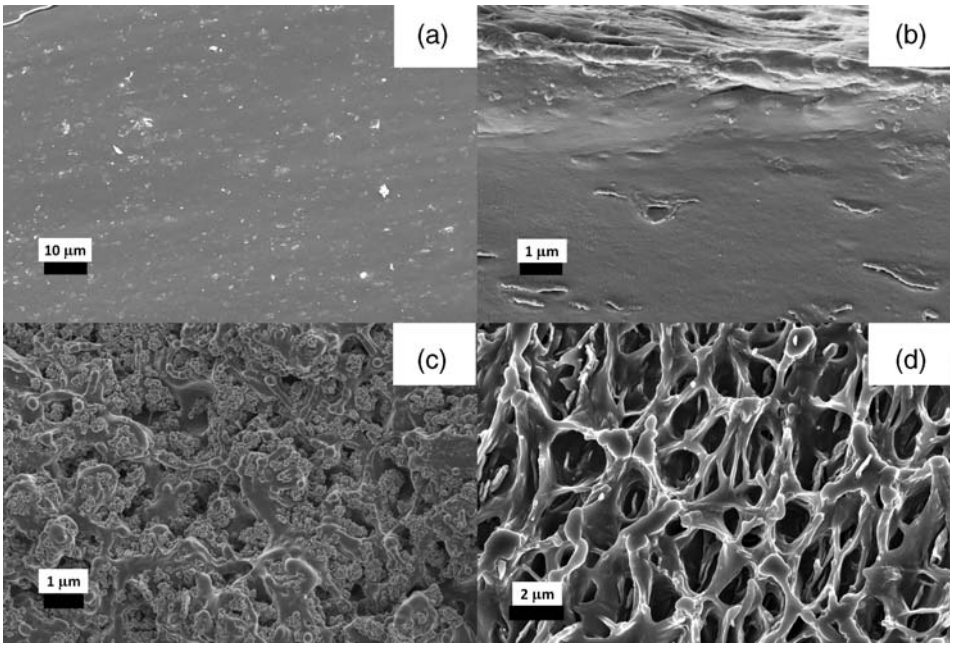

FIGURE 4 Scanning electron micrographs (SEM) of strands after leaching the repellent. (A) Typical outer surface texture featured by all strands. (B) Cryocut cross-section of a strand originally containing 20 wt % Icaridin 5 wt% clay. Fracture surfaces of DEET containing strands with (C) 40 wt% repellent and 5 wt% pyrogenic silica, and (D) 20 wt% repellent and 5 wt% clay

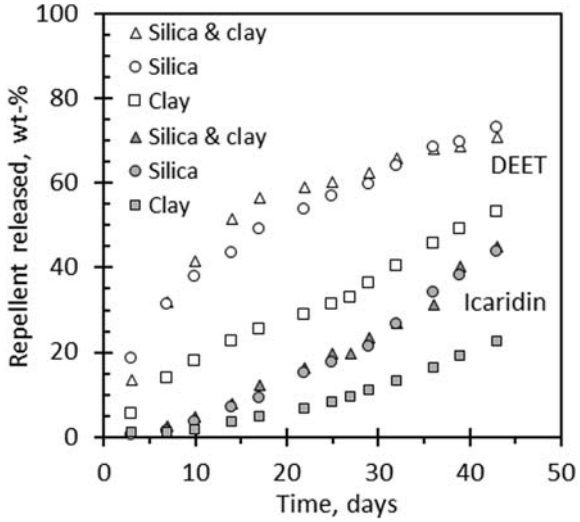

FIGURE 5 The repellent release profiles obtained at 50°C showing the effect of nanofiller type and repellent nature. The fillers were present at the 5 wt% level and the nominal repellent content was 30 wt%

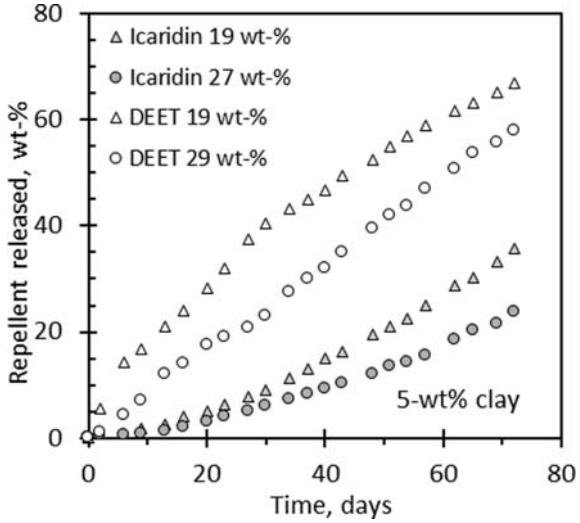

FIGURE 6 The effect of repellent content on release from the EVA strands containing 5 wt% organoclay. The strands had a nominal diameter of 6.1 mm and they were aged in a convection oven set at 50°C

In fact, it always provided an acceptable fit to the experimental data. Therefore, the present results were interpreted based on this model and the exponents are listed in Table 1. The release profiles for the majority of DEET-containing strands featured diffusional exponents that correspond to "anomalous transport". Strands containing low quantities of Icaridin, that is, 20 wt% featured diffusional exponents close to unity meaning that the release rate was approximately zero order. However, samples containing organoclay and nominally 30 wt% or more Icaridin tended to exhibit super Case II release behavior with the diffusional exponent significantly exceeding unity.

Figure 9 illustrates the range of release profile behaviors that were observed. Sample B contained 28 wt% Icaridin and also 5 wt% each of clay and silica yet showed a near zero order release rate. Noteworthy is the Super Case II trends exemplified by sample C. This corresponds to an acceleration of the release rate during the initial stages of the process. Unfortunately, the mechanism responsible for this unexpected behavior is unclear. However, this type of behavior only occurred with Icaridin in

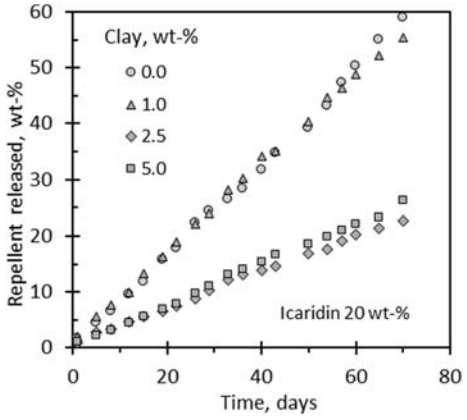

FIGURE 7 The effect of organoclay loading on repellent release from EVA strands with a nominal diameter of 3.1 mm aged in a convection oven set at 50°C

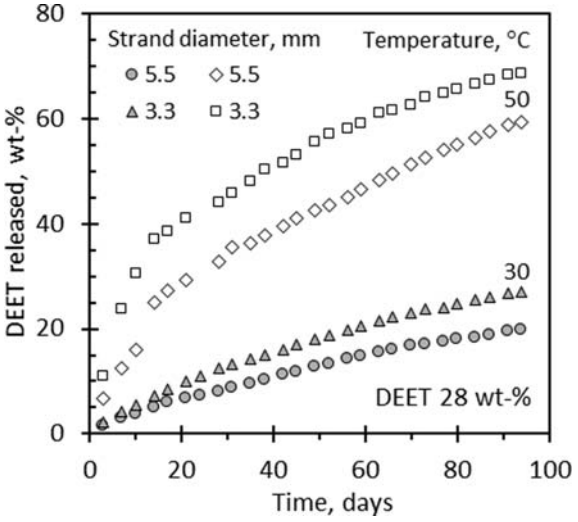

FIGURE 8 Effect of aging temperature and strand diameter on the release of DEET from EVA strands

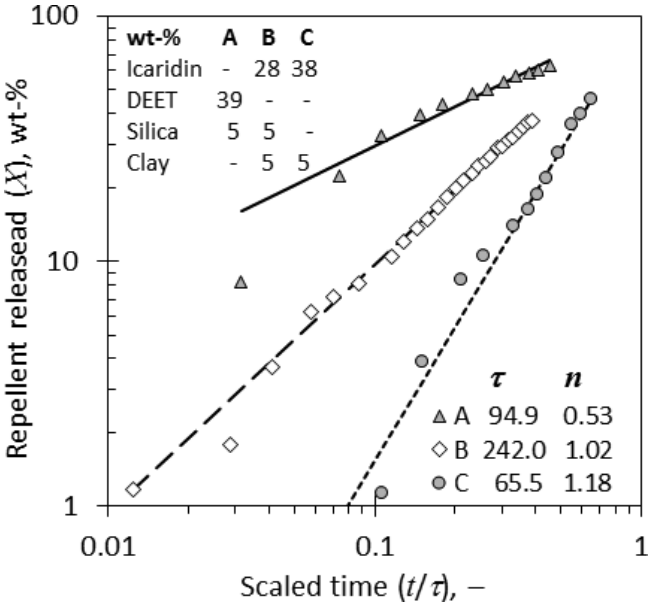

FIGURE 9 Representative release rate fits using the Korsmeyer-Peppas model

combination with organoclay as nanofiller. It could be that there is a special affinity between the organic portion of the clay and the Icaridin itself that, in time, leads to the creation of internal conduits that facilitate rapid transport of the repellent to the outside of the strands.

For DEET samples, the diffusional exponent values ranged from 0.3 to 0.95, indicating Fickian behavior for some samples and, for others, a coupling of Fickian diffusion and a relaxation mechanism. Previous studies reported values for the Weibull shape parameter (n): the internal diffusion mechanism applies for 0.6–0.7; values between 0.9 and 1.0 indicate an external resistance to mass transfer while values higher than 1.0 correspond to the relaxation-controlled mechanism.[16]

Non-Fickian and Case II transport profiles are indicative of the coupling of diffusion and relaxation mechanisms. Relaxation is related to a transition from a rubbery to a glassy state. Major relaxation mechanisms are indicative of stresses formed in the polymer during swelling.[18]

The present results are in agreement with those observed by Marabi, Livings, Jacobson and Saguy[18] and Cunha, Oliveira, Ilincanu and Drumond,[16] where the utilization of the Weibull distribution showed excellent fit for the description of rehydration of a variety of dried foods and adequately described rehydration processes controlled by different mechanisms, which included internal diffusion, external convection and relaxation.

5 | CONCLUSION

EVA nanocomposite strands filled with the mosquito repellents DEET or Icaridin were prepared by an extrusion-compounding process. The compounding process was facilitated by the presence of pyrogenic silica and/or organoclay Dellite 43B at the 5 wt% level. All strands featured a relatively smooth outer surface, but the internal morphology varied from dense to highly porous. The repellent release profiles were determined by oven aging at 30 and 50°C in convection ovens. DEET was released significantly faster than Icaridin. Release rate was faster with nanosilica than with clay, with higher repellent loadings compared to lower loadings, and for thinner strands compared to thicker ones. EVA swelled slightly (close to 5%) and, consequently, it shrank when the repellent was released. This effect can cause

poor dimensional stability. However, EVA can still be considered for end-use application because of its high flexibility derived from its rubbery nature. The Korsmeyer-Peppas power law model adequately described the repellent release profiles. The values assumed by the diffusional exponent (n) in this model are associated with different transport mechanisms. Release from some DEET-containing strands were consistent with Fickian diffusion but for most of them, the release could be described as anomalous, that is, in-between Fickian diffusion and relaxational transport. Strands containing the organoclay and low levels of Icaridin featured the desired zero order release rate behavior. However, strands with high loadings of Icaridin showed Super Case II repellent release. These observations showed that the models provided valuable insights, clarifying the mechanism by which the repellents were released from the swellable EVA matrix strands. It was possible to differentiate between diffusion and relaxation mechanisms.

ACKNOWLEDGMENTS

This work was supported by the Deutsche Forschungsgemeinschaft (DFG) [Grant AN 212/22-1]. Saltigo (Germany) is thanked for the generous gift of Saltidin samples and Laviosa Chimica Mineraria S.p.A (Italy) for providing the Dellite 43B organoclay sample.

DATA AVAILABILITY STATEMENT

The data that supports the findings of this study are available in the supplementary material of this article

ORCID

Alcides Sitoe https://orcid.org/0000-0001-8781-3378

REFERENCES

[1] S. B. Murugan, R. Sathishkumar, *Asian Pac. J. Trop. Med.* **2016**, *9*(10), 933.
[2] D. M. Morens, A. S. Fauci, *J. Infect. Dis.* **2016**, *214*(suppl_5), S434–S435.
[3] G. Benelli, *Asian Pac. J. Trop. Biomed.* **2016**, *6*(4), 353.
[4] R. De Jong, B. Knols, *Experientia* **1995**, *51*(1), 80.
[5] L. Braack, R. Hunt, L. L. Koekemoer, A. Gericke, G. Munhenga, A. D. Haddow, P. Becker, M. Okia, I. Kimera, M. Coetzee, *Parasit. Vectors* **2015**, *8*, 76.
[6] A. B. Mapossa, M. M. Sibanda, A. Sitoe, W. W. Focke, L. Braack, C. Ndonyane, J. Mouatcho, J. Smart, H. Muaimbo, R. Androsch, *Chem. Eng. J.* **2019**, *360*, 435.
[7] M. U. Akhtar, W. W. Focke, *Thermochim. Acta* **2015**, *613*, 61.
[8] R. S. Langer, N. A. Peppas, *Biomaterials* **1981**, *2*(4), 201.
[9] C. Schneider, R. Langer, D. Loveday, D. Hair, *J. Controlled Release* **2017**, *262*, 284.
[10] A. Almeida, S. Possemiers, M. N. Boone, T. De Beer, T. Quinten, L. Van Hoorebeke, J. P. Remon, C. Vervaet, *Eur. J. Pharm. Biopharm.* **2011**, *77*(2), 297.
[11] Y. Fu, W. J. Kao, *Expert Opin. Drug Deliv.* **2010**, *7*(4), 429.
[12] N. Genina, J. Hollander, H. Jukarainen, E. Makila, J. Salonen, N. Sandler, *Eur. J. Pharm. Sci.* **2016**, *90*, 53.
[13] J. A. H. van Laarhoven, M. A. B. Kruft, H. Vromans, *J. Controlled Release* **2002**, *82*(2), 309.
[14] W. D. Rhine, D. S. T. Hsieh, R. Langer, *J. Pharm. Sci.* **1980**, *69* (3), 265.
[15] N. A. Peppas, N. M. Franson, *J. Polym. Sci., Polym. Phys. Ed.* **1983**, *21*(6), 983.
[16] L.M. Cunha, F.A.R. Oliveira, L.A. Ilincanu, M.C. Drumond, Application of the probabilistic Weibull model to rehydration kinetics: relationship between the model parameters and the underlying physical mechanisms, Process Optimization and Minimal Processing of Foods, 1998, pp. 9–13.
[17] L. M. Cunha, F. A. R. Oliveira, J. C. Oliveira, *J. Food Eng.* **1998b**, *37*(2), 175.
[18] A. Marabi, S. Livings, M. Jacobson, I. S. Saguy, *Eur. Food Res. Technol.* **2003**, *217*(4), 311.
[19] L. Brannon-Peppas, N. A. Peppas, *J. Controlled Release* **1989**, *8* (3), 267.
[20] C. S. Brazel, N. A. Peppas, *Eur. J. Pharm. Biopharm.* **2000**, *49* (1), 47.
[21] G. W. R. Davidson, N. A. Peppas, *J. Controlled Release* **1986**, *3* (1), 243.
[22] G. W. R. Davidson, N. A. Peppas, *J. Controlled Release* **1986**, *3* (1), 259.
[23] D. Hariharan, N. A. Peppas, R. Bettini, P. Colombo, *Int. J. Pharm.* **1994**, *112*(1), 47.
[24] R. S. Harland, N. A. Peppas, *Polym. Bull.* **1987**, *18*(6), 553.
[25] R. S. Harland, N. A. Peppas, *Colloid Polym. Sci.* **1989**, *267* (3), 218.
[26] H. B. Hopfenberg, K. C. Hsu, *Polym. Eng. Sci.* **1978**, *18*(15), 1186.
[27] J. Klier, N. A. Peppas, *J. Controlled Release* **1988**, *7*(1), 61.
[28] R. W. Korsmeyer, S. R. Lustig, N. A. Peppas, *J. Polym. Sci., Part B: Polym. Phys.* **1986**, *24*(2), 395.
[29] R. W. Korsmeyer, E. Von Meerwall, N. A. Peppas, *J. Polym. Sci., Part B: Polym. Phys.* **1986**, *24*(2), 409.
[30] S. R. Lustig, N. A. Peppas, *J. Appl. Polym. Sci.* **1987**, *33*(2), 533.
[31] K. V. R. Rao, K. P. Devi, *Int. J. Pharm.* **1988**, *48*(1), 1.
[32] C. M. Walker, N. A. Peppas, *J. Appl. Polym. Sci.* **1990**, *39*(10), 2043.
[33] P. L. Ritger, N. A. Peppas, *J. Controlled Release* **1987b**, *5*(1), 37.
[34] P. L. Ritger, N. A. Peppas, *J. Controlled Release* **1987a**, *5*(1), 23.
[35] N. A. Peppas, J. J. Sahlin, *Int. J. Pharm.* **1989**, *57*(2), 169.
[36] R. W. Korsmeyer, R. Gurny, E. Doelker, P. Buri, N. A. Peppas, *Int. J. Pharm.* **1983**, *15*(1), 25.
[37] Y. Danyuo, C. Ani, A. Salifu, J. Obayemi, S. Dozie-Nwachukwu, V. Obanawu, U. Akpan, O. Odusanya, M. Abade-Abugre, F. McBagonluri, *Sci. Rep.* **2019**, *9*(1), 1.
[38] W. W. Focke, I. Van der Westhuizen, N. Musee, M. T. Loots, *Sci. Rep.* **2017**, *7*(1), 1.
[39] V. Papadopoulou, K. Kosmidis, M. Vlachou, P. Macheras, *Int. J. Pharm.* **2006**, *309*(1–2), 44.
[40] S. Dash, P. N. Murthy, L. Nath, P. Chowdhury, *Acta Pol. Pharm.* **2010**, *67*(3), 217.
[41] M.-L. Mateus, C. Lindinger, J.-C. Gumy, R. Liardon, *J. Agri. Food Chem.* **2007**, *55*(25), 10117–10128.
[42] J. Balcerzak, M. Mucha, *Prog. Chem. Appl. Chitin Its Deriv.* **2010**, *15*, 117.

[43] Z. N. Charara, J. W. Williams, R. H. Schmidt, M. R. Marshall, *J. Food Sci.* **1992**, *57*(4), 963.
[44] B. Troitskii, G. Razuvaev, L. Khokhlova, G. Bortnikov, *J. Polym. Sci.: Polym. Symp.* **1973**, *42*(3), 1363.
[45] M. Zanetti, G. Camino, R. Thomann, R. Mülhaupt, *Polymer* **2001**, *42*(10), 4501.

SUPPORTING INFORMATION

Additional supporting information may be found online in the Supporting Information section at the end of this article.

How to cite this article: Sitoe A, Mapossa AB, Focke WW, Muiambo H, Androsch R, Wesley-Smith J. Development, characterization and modeling of mosquito repellent release from microporous devices. *SPE Polymers*. 2020;1:90–100. https://doi.org/10.1002/pls2.10021